(NASA-CR-157324) STUDY OF CHANGES IN PROPERTIES OF SOLAR SAIL MATERIALS FROM RADIATION EXPOSURE Final Report, 2 Jun. - 29 Nov. 1977 (Rockwell International Corp., Thousand Oaks) 26 p HC A03/MF A01 CSCL 22B G3/18

N78-28161

Unclas 25964

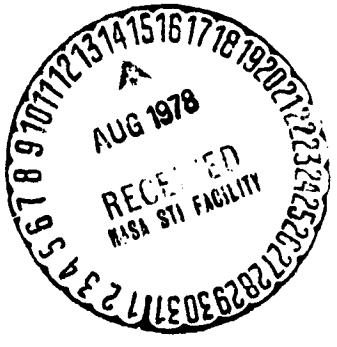

SC5114.7FR

STUDY OF CHANGES IN PROPERTIES OF SOLAR SAIL MATERIALS FROM RADIATION EXPOSURE

FINAL REPORT

For period 6/2/77 through 11/29/77

Subcontract No. 954776

General Order No. 5114

Prepared for:

California Institute of Technology
Jet Propulsion Laboratory
Pasadena, CA 91103

November 1977

T. Smith

Tennyson Smith
Principal Investigator

Rockwell International
Science Center

OBJECTIVE

The objective of this study is to develop techniques for monitoring changes in preparation of solar sail materials resulting from space radiation simulation, stressing (e.g., thermal, mechanical) and exposure to terrestrial environments. JPL is interested in testing the suitability of various solar sail materials for the Halley's comet tracking mission. The properties of interest are: metallic coating deterioration, polymeric film deterioration, interfacial debonding and possible metallic coating diffusion into the polymeric film.

METHODOLOGY

Four accelerated tests have been devised to simulate the possible degradation processes mentioned above. These four tests are: a thermal shock test to simulate the wide variation of temperature expected in space (260°C to -100°C), a cyclic temperature test to simulate the 6 minute temperature cycle anticipated in space, a mechanical vibration test to simulate mechanical bonding, folding and handling, and a humidity test to simulate terrestrial environment effects. All of these tests are considerably more extreme than anticipated for the solar sail in order to accelerate the degradation processes.

The techniques for monitoring property changes are: visual and microscopic examination, ellipsometry, surface potential difference (SPD), photoelectron emission (PEE), and water contact angles. The surface tools, SPD, PEE and contact angle are very surface sensitive and relate to changes that might affect reflectivity and emissivity due to corrosion and mechanical stresses. The ellipsometer is surface sensitive but is also sensitive to changes at the metal-polymer interface due to delamination.

The measurements from the nondestructive tools are correlated with a destructive peel test to directly monitor adhesion degradation at the aluminum-polymer interface by the radiation exposure (at Boeing) as well as the accelerated tests at the Science Center.

EXPERIMENTAL RESULTS

A. Surface Characterization

The surface tools have been described in a previous paper[1] (copy enclosed). Table 1 is an inventory of samples from JPL. Table 2 gives initial ellipsometric parameters (Δ, ψ), SPD, PEE and θ_{H_2O} of the materials on the aluminum and on the chromium sides.

The Δ and ψ values for the aluminum side correspond to ~100Å of oxide on aluminum for $\Delta = 134^{o}$ and ~200Å oxide for $\Delta = 126^{o}$. The ψ values indicate the aluminum is very smooth. The values of Δ for the chromium side correspond to about 30Å of oxide on chromium for the 155-200Å layer. The larger Δ value for 50Å of chromium indicates the light sees through to the Kapton substrate. The ψ values do not correspond to oxides on smooth chromium and may indicate the chromium is very rough or granular. The large variations of Δ and ψ for the Kapton indicate the light is seeing through the transparent Kapton to the metal films. Looking through Kapton to aluminum gives $\Delta \sim 340^{o}$, looking through to chromium gives $\Delta \sim 5\text{-}20^{o}$. The Δ values for Ag on Al corresponds to about 30Å of oxide or sulfide on silver, but again the ψ value does not correspond to smooth silver. The Δ and ψ values for MgF_2/Al correspond to 2600Å rather than 200Å.

1. T. Smith, J. Appl. Phys. 46, 1553 (1975).

TABLE 1

INVENTORY OF SAMPLES ON HAND FROM JPL

JPL No.	Coating	Method	Substrate	Thickness	Size (in.)	Comment
207A	1000Å Al, 50Å Cr	ion	Kapton	0.3 mil	3x5 & 2x3	
210	1000Å Al, 200Å Cr	ion	Kapton	0.3	3x3 & 1x2	Al is "patchy"
215	300Å Ag over 700Å Al	ion	Kapton	0.3	5x6 & 2x2	Coating is one side only
212A	200Å MgF_2 over 1000Å Ag	ion	Kapton	0.3	5x4 & 3x3	
212B	200Å MgF_2 over 1000Å Ag	ion	Kapton	0.3	4½ x 8	Looks "blotchy"
164 RSC	1000Å Al	vapor	Kapton	0.3	10 x 12	
166	155Å Cr	vapor	Kapton	0.3	10 x 12	
167A RSC	155Å Cr	vapor	Kapton	0.1	6x10 & 5x2	(measures ~ 0.2 mil)
167B(X)	155Å Cr	vapor	Kapton	0.1	6x10 & 6x2	(measures ~ 0.2 mil)
XXX	1000Å Al	vapor	Kapton	0.1	3x3½ & 3x3½	(measures ~ 0.2 mil)
(Prelim. Boeing)	1000Å Al, 150Å Cr		CGS*	0.1	1x3½	(measures ~ 0.3 mil
341	None	-	Kapton	0.3	6x8	
342	1000Å Al, 125Å Cr		Kapton	0.1	2x4 & 1½ x 2	Bench mark
Pro-Kapton	Al & Cr, 1000Å & 150Å		Kapton	0.1	2¼ x 3	(measures ~ 0.2 mil)
Pro-CGS	1000Å Al, 150Å Cr		CGS	0.1	2¼ x 3¼	
Pro-Kapton	150Å Cr		Kapton	0.1	3x3	(measures ~ 0.2 mil)
Pro-CGS	150Å Cr		CGS	0.1	3x3	
Pro-CGS	1000Å Al		CGS	0.1	3x3	
Pro-Kapton	1000Å Al		Kapton	0.1	3x3	(measures ~0.2.mil)
Ad Joint Test	-	-	-	-	6½x9	
382	1000Å Al		Kapton	0.1	6x12	
499	1000Å Al		Kapton	0.1	9x12	
498	1000Å Al (oxidized)		Kapton	0.1	6x6	
165	1000Å Al		Kapton	0.1	6x12	

*Ciba Geigy Substrate

TABLE 2

INITIAL SURFACE PROPERTIES OF SOLAR SAIL FILMS

Sample No.	Description	Side	Δ (deg)	ψ (deg)	SPD (volts)	PEE (amps x 10^{11})	θ_{H_2O} (deg.)
207A	1000Å Al 0.3 Kapton-50Å Cr	Al	134.0	41.9	1.0	400	87
210	1000Å Al 0.3 Kapton-200Å Cr	Al	134.0	42.1	0.95	320	87
164 RSC	1000Å Al 0.3 Kapton-no Cr	Al	125.9	41.4	1.0	400	98
(Prelim. Boeing)	1000Å Al 0.1 CGS-150Å Cr	Al	126.1	41.2	1.0	350	90
Pro-Kapton	1000Å Al 0.1 Kapton-KOH etched	Al	132.5	41.8	1.0	450	91
Bench mark 342	1000Å Al 0.1 Kapton-125Å Cr	Al	126.7	40.3	0.8	400	71
207A	1000Å Al 0.3 Kapton-50Å Cr	Cr	176.4	36.5	0.07	50	85
210	1000Å Al 0.3 Kapton-200Å Cr	Cr	124.6	20.8	0.17	120	80
166	No Al 0.3 Kapton-155Å Cr	Cr	119.8	15.5	0.18	150	98
167A RSC	No Al 0.1 Kapton-155Å Cr	Cr	122.1	18.1	0.28	150	98
167B(X)	No Al 0.1 Kapton-155Å Cr	Cr	124.1	19.0	0.24	120	98
Pro-Kapton	1000Å Al 0.1 Kapton-no Cr	Kapton	349.1	19.4	-	-	70
166	No Al 0.3 Kapton-155Å Cr	Kapton	22.6	11.4	-	-	72
167A RSC	No Al 0.1 Kapton-155Å Cr	Kapton	66.6	3.5	-	-	77
164 RSC	1000Å Al 0.3 Kapton-No Cr	Kapton	336.2	4.9	-	-	45
167B(X)	No Al 0.1 Kapton-155Å Cr	Kapton	5.0	5.2	-	-	76
341	No Al.0.1 Kapton-155Å Cr	Kapton	4.4	13.6	-	-	73
215	Ion plate, 300Å Ag/700Å Al	Ag	110.4	34.9	0.0	450	100
212A	Ion plate, 200Å MgF_2/1000Å Al	MgF_2	208.9	41.55	-0.04	200	30

The absolute value of SPD has no significance because it is the difference in work function between the sample and a reference electrode. There is significance to the difference between SPD values from one sample to another or for the same sample that is changing surface properties. The aluminum layer consistently yields SPD ~1 volt and chromium ~0.17-0.28 volts (except for the 50Å layer). Silver yields SPD ~0.0 volts and MgF_2 ~-.04 volts.

Reproducible but different PEE values result for each type of surface. Aluminum yields an emission current of ~400 x 10^{-11} amps as does silver. Chromium yields PEE ~120-150 x 10^{-11} amps (except for the thin 50Å layer). The MgF_2 attenuates emission from the Al to 200 x 11^{-11} amps.

The metal surfaces are very active upon exposure to the atmosphere and the oxide layer strongly adsorbs organic contamination. The polar end or part of the organic contamination is bonded to the oxide leaving the nonpolar part at the outer surface. This low energy surface yields water contact angles of 80-90° as compared to ~70° for the Kapton and ~30° for polar MgF_2.

Thermal Shock Test

Samples of 0.3 mil Kapton, with (sample No. 207A) and without (No. 164) chromium were subjected to two or three dips into liquid nitrogen from room temperature and from 220°C to simulate large temperature cycles that will occur in space (although the transient time in space will be extremely long in comparison to our test). Table 3 shows that no significant changes in surface parameters occurred and no visible damage was observed. The experiment was repeated with 0.1 mil Kapton with similar results.

TABLE 3

SURFACE PROPERTIES FOR THERMALLY SHOCKED SOLAR SAIL FILMS*

Sample No	Treatment	Side	Δ (deg)	ψ (deg)	SPD (volts)	PEE (amps x 10^{11})	θ_{H_2O} (deg)
164	Prior to shock	Al	125.9	41.4	1.0	400	98
164	2 cycles in Liquid N_2	Al	127.6	41.5	0.95	500	95
164	220°C 10 min., Liquid N_2	Al	126.0	41.3	-	-	-
164	220°C 10 min., Liquid N_2	Al	127.0	41.5	-	-	-
207A	Prior to shock	Al	134.0	41.9	1.0	400	87
207A	2 cycles in Liquid N_2	Al	134.3	41.9	0.95	400	81
207A	220°C 10 min., Liquid N_2	Al	133.5	41.9	-	-	-
207A	220°C 10 min., Liquid N_2	Al	133.0	42.0	-	-	-

* No visible damage after these treatments.
The experiment was repeated with 0.1 mil material, no damage resulted.

Thermal Cycle Test

To simulate the thermal stress expected in space with a 6 min. period, samples were placed in a revolving wheel (see Fig. 1) that passed through two halves of a clam shell furnace. The samples spent approximately two minutes at 260°C then cooled to room temperature before entering the furnace zone again.

The CGS Boeing sample had a burned appearance after a few cycles. The border of the sample, that was enclosed in aluminum foil of the holder, appeared unchanged (probably did not reach temperature) whereas the aluminum side exposed to the air appeared white as though it were oxidized and the chromium side appeared colored as though it were oxidized. The sample had a shrivelled appearance. The rest of the samples subjected to this test are reported in Table 4. Visual or microscopic observation of the aluminum side revealed no apparent change in the samples after 1630 cycles or 2400 cycles. However, every sample showed changes in surface properties.

The aluminum has added about 30Å of oxide after 1400 cycles. After 2400 cycles Δ and ψ cannot be interpreted in terms of oxidation alone. The Δ and ψ values after temperature cycling indicates that much of the chromium has been removed or oxidized and this is verified by visual observation. The SPD is changed in almost every case and, except for 207C, the PEE for Al increases with cycling. SPD and PEE are not measured on Kapton alone due to its insulating properties. Temperature cycling reduces θ_{H_2O} for the metals due to oxidation that removes organic contamination. For Kapton θ_{H_2O} remains approximately constant as might be expected.

Mechanical Vibration Test

Samples of 207A were placed in a jig (see Fig. 2) with the ends fixed and the center vibrated at 40 Hz and approximately 0.5 cm amplitude to act as an accelerated

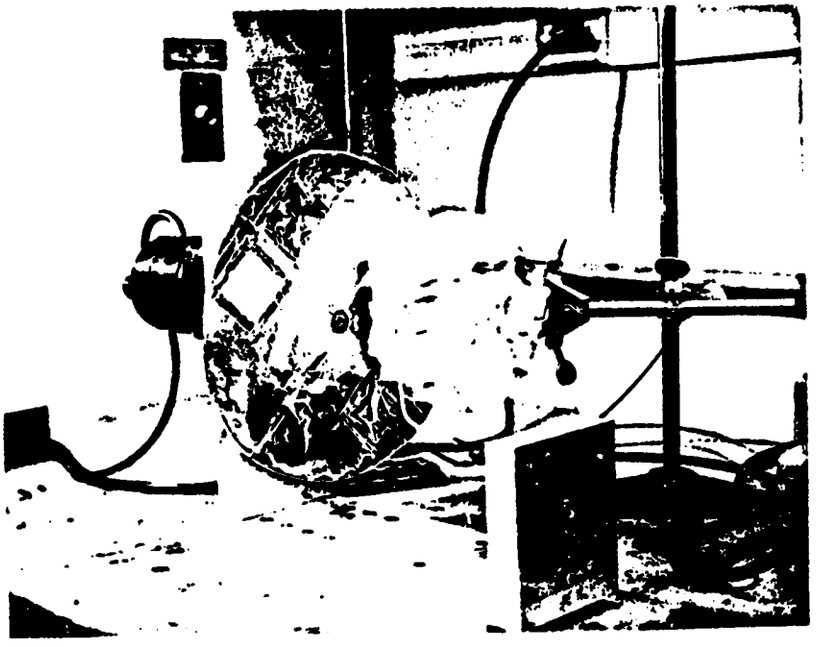

Fig. 1. Apparatus for thermal cycling of solar sail material.

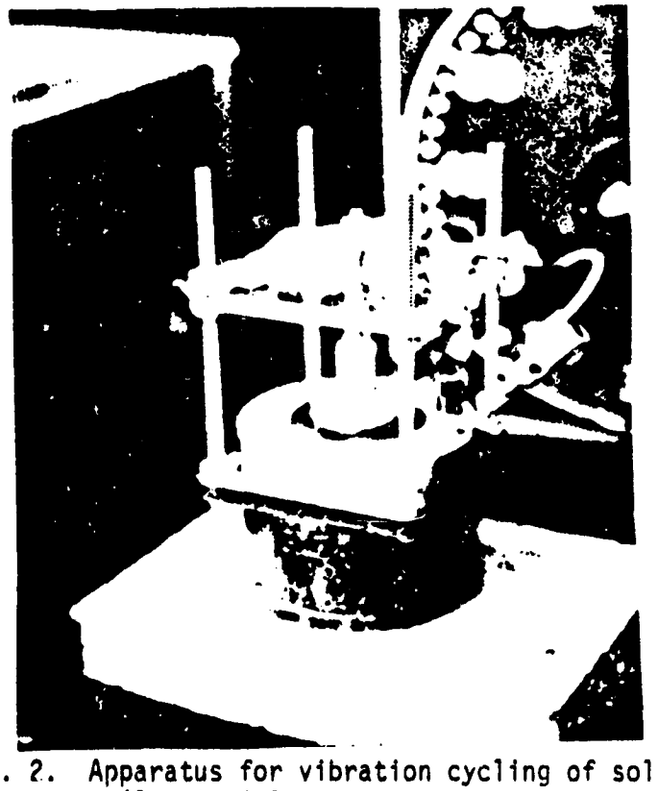

Fig. 2. Apparatus for vibration cycling of solar sail material

TABLE 4

SURFACE PROPERTIES OF THERMALLY CYCLED MATERIAL*

Sample No.	Treatment	Side	Δ (deg)	Ψ (deg)	SPD (volts)	PEE (amps x 10^{11})	θ_{H_2O} (deg)
210	Prior	Al	134.0	42.1	0.95	320	87
210	1440 cycles, 6 min.period	Al	130.7	41.7	0.60	500	30
210	Prior	Cr	124.6	20.8	0.17	120	30
210	1440 cycles, 6 min. period	Cr	108.8	21.2	-0.2	45	31
207C	Prior	Al	134.0	41.9	1.0	400	87
207C	1630 cycles, 6 min period	Al	132.9	42.0	0.7	300	29
207C	Prior	Cr	176.4	36.5	0.07	50	85
207C	1630 cycles, 6 min. period	Cr	339.8	23.9	-	-	11
342	Prior	Al	124.4	40.7	0.48	140	51
342	2400 cycles, 6 min. period	Al		40.0	0.56	480	15
342	Prior	Cr	148.8	20.3	0.10	80	91
342	2400 cycles, 6 min. period	Cr	335.5	5.1	0.45	120	28
XXX	Prior	Al	132.5	41.6	0.54	200	85
XXX	2400 cycles, 6 min. period	Al	41.2	41.2	0.54	600	24
XXX	Prior	Kapton	299.4	47.3	-	-	52
XXX	2400 cycles, 6 min. period	Kapton	2.2	16.5	-	-	58
167B	Prior	Kapton	348.5	10.5	-	-	78
167B	2400 cycles, 6 min. period	Kapton	136.5	12.0	-	-	64

* Except for CGS Boeing sample, no visible damage to any of these samples.

test of stresses due to flexuring the sail material. After 192 hrs (28×10^6 cycles) of flexure, no visible change was observed. However, Table 5 shows that changes in surface properties had occurred. On the aluminum side Δ and ψ correspond to about 100Å of oxide growth and PEE and θ_{H_2O} are dramatically decreased. The chromium side had large changes in Δ and ψ but minor changes in SPD, PEE and θ_{H_2O}. The values were closer to that for Kapton, as though some of the Cr has been removed.

Peel Test

It was initially recognized that a direct destructive degradation test is needed to correlate with nondestructive inspection techniques. A good degradation test would be the failure of the aluminum film to adhere to the Kapton. Delamination could occur from degradation of the Kapton-aluminum interfaces or degradation of the entire Kapton film. Degradation is considered to be anything that would change the optical properties or the mechanical strength or adhesive properties of the laminations in the sail under anticipated environmental conditions. These conditions include mechanical handling, exposure to humid atmospheres prior to launch, exposure to sunlight before and after launch, exposure to thermal stresses before and after launch, etc.

We have developed a peel test that will measure the force necessary to delaminate the aluminum film from the Kapton. The difficulty associated with this test, as well as for making NDI surface measurements, is in handling the flimsy material, which curls up and blows away at every opportunity. We have been able to make smooth flat samples for NDI measurements by placing samples on wet microscope cover glass slides.

TABLE 5

SURFACE PROPERTIES OF MECHANICALLY CYCLED MATERIAL*

Sample No.	Treatment	Side	Δ (deg)	ψ (deg)	SPD (volts)	PEE (amps x 10^{11})	θ_{H_2O} (deg)
207A	Prior	Al	134.0	41.9	1.0	400	87
207A	Vibrate 40 Hz, 192 hrs.	Al	127.0	42.0	0.8	80	62
207A	Prior	Cr	176.4	36.5	0.07	50	85
207A	Vibrate 40 Hz, 192 hrs.	Cr	12.3	53.0	0.0	68	80

* No visible change, even under 30 power microscope.

To provide a wrinkle free peel specimen that will fail at the Kapton - (1000Å Al) interface, the following procedure has been developed.

1. Press the sail material on to a wet cover glass with the aluminum side adjacent to the glass (wrinkle free).

2. Press 5 minute epoxy between the sail material and another clean (dust free) cover slide until a uniform layer of epoxy is formed.

3. Remove the wet cover slide and surface treat the 1000Å Al for bonding (see next section).

4. Press 5 minute epoxy between clean Kapton (acetone wiped, 1 mil), and squeegy back and forth until a uniform layer of epoxy is formed and the sail material is wrinkle free.

5. Slice the Kapton-epoxy-sail-epoxy layer into 0.2 cm strips and peel back the strips. Place the glass slide in one of the Instron grips and attach an adhesive tape between the peel strip and the other grip to make 180° peel.

With this procedure, in most cases, the aluminum will be peeled off the Kapton-sail material and transferred to the epoxy. The narrow (0.2 cm) strips are used, rather than the standard 1" strips, because the samples from the radiation (Boeing) test will only be about 1" x ½". Figure 3a shows a peel specimen in the Instron and Fig. 3b shows a closer view.

Table 6 gives initial results of the peel test for sample No. 382 (0.1 mil Kapton) dry, after 1 hr. at 95% RH and 60°C and with a drop of water on the peel crack. Strips 1, 3, 4, 5, 7, 10 and 11 gave reproducible results of ~35 g/cm (0.2#/in). Exposure to 95% RH and 60°C for 1 hr reduced the peel strength by 50%. Note that the drop in peel strength was uniform along the strip rather than near the peeled

TABLE 6

RESULTS OF INITIAL PEEL TESTS OF SOLAR SAIL MATERIAL
(Peel Rate 0.5 cm/min, Peel Strip 0.2 in. wide)

Test	Average Peel Force					
	Dry		Humidity test 1 hr, 95% RH, 60°C		Liquid Water	
	g/cm	lb/in	g/cm	lb/in	g/cm	lb/in
1	35	0.2	18	0.10	-	-
3	35	0.2	15	0.08	-	-
4	35	0.2	15	0.08	5	0.03
5	35	0.2	-	-	10	0.06
7	35	0.2	-	-	-	-
10	35	0.2	15	0.08	-	-
11	35	0.2	-	-	-	-
2	50	0.28	25	0.14	-	-
6	60	0.34	-	-	5	0.03
8	-	-	35	0.20	-	-
9	65	0.36	25	0.14	5	-

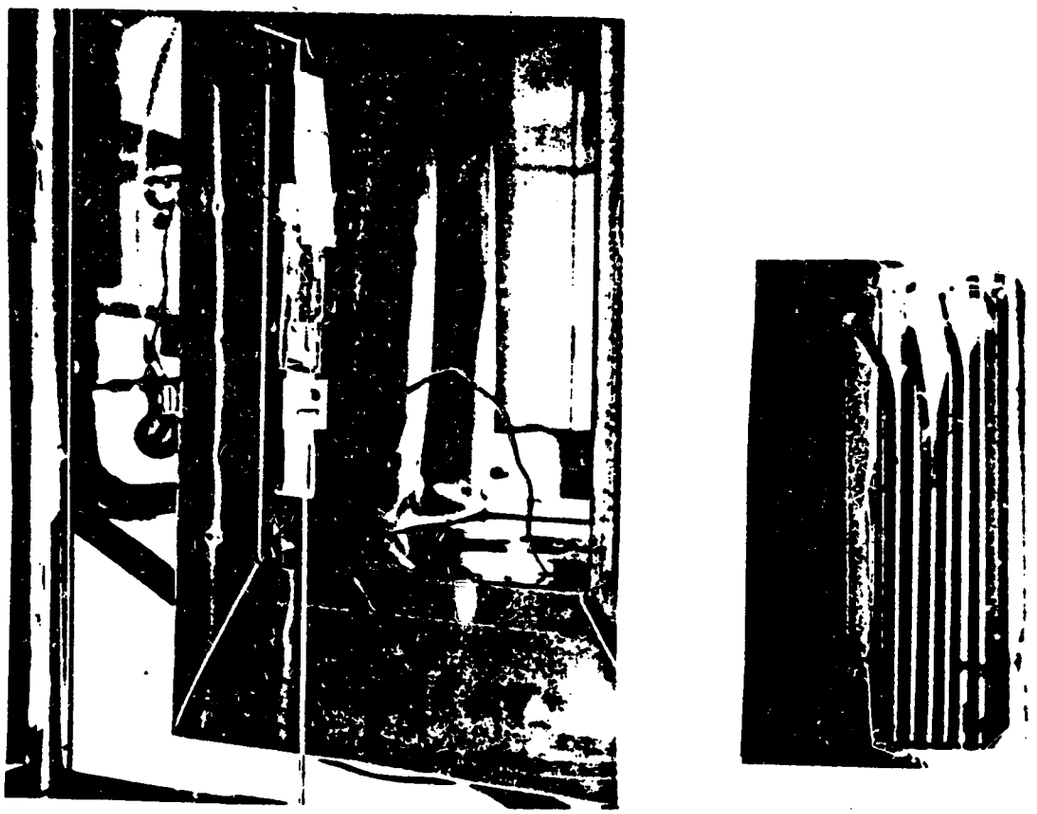

(a) (b)

Fig. 3. (a) Peel specimen in the Instron
(b) Peel specimen

back region. Either moisture penetrates at the edges along the strip or through the Kapton. We will check this by exposing to moisture before slicing the strips. Liquid water at the crack tip decreases the peel strength by about 70-80%. Strips 2, 6, and 9 gave larger peel strength due to nonuniform epoxy thickness. Note that the percent reduction in peel strength due to the humidity test is approximately the same as for the other strips (~50%).

Surface Preparation

To provide peel test samples, it is necessary to bond a backup strip to the aluminum on the Kapton such that failure is at the aluminum-Kapton interface. Adhesive bonding of aluminum foil or other backup material fails because the aluminum - on Kapton is contaminated with organic material (θ_{H_2O} ~90^o). It therefore becomes necessary to surface treat the sail material. Conventional surface treatments, such as acid or alkaline etching completely destroys the 1000Å layer. We have obtained excellent bonding by a modified STAB process. STAB stands for surface treatment of aluminum for bonding, a process developed at the Science Center. This treatment is the most simple one yet developed and involves only soaking the sample in 80^oC aqueous carbonate solution for 10 minutes. In the case of the solar sail 10 minutes will convert the entire 1000Å to hydroxide, but 1 min. only converts a few hundred angstroms and yet provides a good bond.

We have noted that the adhesively bonded sheets of sail material have good shear strength but essentially no peel strength. The overlap strips peel off about as easily as if water is used as the adhesive. This is because of the contaminated aluminum surface which cannot be adequately cleaned by degreasing.

The modified STAB process may well prove to be the only simple way of preparing the aluminum for bonding. If it is not feasible to dip sail sheets in hot water, it may be possible to expose the regions to be bonded to hot water by a sponge technique.

Ultrasonic Test

It was discovered that exposure of sail material to ultrasonic exitation, in an ultrasonic degreasing unit, caused the aluminum to delaminate. Figure 4a shows a photograph of sail material, with light source below, prior to ultrasonic exposure and Fig. 4b after ultrasonic exposure. The light transmitted through the material where the aluminum has spalled off. This could be used as a test for the bond strength or durability if a calibration is made of the amount spalled off per unit time in the ultrasonic equipment.

Irradiated Samples

A control sample and two irradiated samples were investigated to reveal radiation effects. One sample was irradiated to 10^3 rads and the other to 10^9 rads over a 1" diameter circular area. Examination with ellipsometry and with the peel test revealed no differences between the irradiated vs the unirradiated regions. The peel force was in the range for the control samples in Table 6 (i.e. 30-60 g/cm).

a b

FIG. 4 a) Transmission photograph of sail prior to ultrasonic test.

b) Transmission photograph of sail after ultrasonic test.

CONCLUSIONS

1. Use of the combined techniques uniquely characterize each surface of the sail material as well as the Kapton-aluminum interface. The surface characterization changes with some of the degradation processes, e.g., thermal cycling, vibration cycling, but these changes have yet to reveal physical degradation that would occur under anticipated solar sail conditions. In fact, visual observation indicates the sail material to be very stable to drastic thermal and mechanical shock or cycling. However, the surface tools indicate partial removal of the chromium layer which can be observed visually in some cases and not in others.

2. We have been able to develop a peel test that removes the aluminum film from the Kapton, and this test reveals interfacial degradation upon exposure to humid and water environments.

3. We have developed a surface treatment that may prove valuable for bonding sail sheets together. This may be important since the present adhesive technique leaves the overlap strip with good shear strength but essentially no peel strength. A disclosure of invention is being filed on this surface treatment methodology.

4. No visual, ellipsometric or peel test difference was observed between irradiated regions (to 10^9 rads) and unirradiated regions of sail material.

Photoelectron emission from aluminum and nickel measured in air

Tennyson Smith

Science Center, Rockwell International, Thousand Oaks, California 91360
(Received 24 October 1974, in final form 23 December 1974)

Photoelectron emission from Al and Ni has been performed under atmospheric conditions. Measurements of photoemission current I, as a function of oxide thickness yield attenuation lengths of 28 Å for Al_2O_3/Al and 71 Å for NiO/Ni for $\lambda = 2500$ Å (~5 eV). Photoemission from Al_2O_3/Al originates at the metal and is only attenuated by the oxide unless the oxide is bombarded with Ar^+. After ion bombardment the oxide also emits electrons. Photoemission from NiO/Ni originates from the oxide for $\lambda = 2500$ Å. Estimates of oxide film thickness can be made for very thin films (0~200 Å) by very simple photoemission measurments in air.

PACS numbers: 79.60.G

INTRODUCTION

Photoelectron emission experiments are usually performed in a vacuum system in order to measure electron current without the hindrance of gas molecules. However, it is convenient and desirable in many instances to measure photoemission under ambient conditions. In these cases, photoemission can be used as a tool for characterizing surfaces.

For films that are transparent to the light, emission occurs from the metal; the film only attenuates emission. In this case, information is gleaned about the metal as well as about the film attenuation properties. This is the case for aluminum oxide on aluminum, as shown in this study for uv light (λ ~2500 Å). For films that are photoemitting in themselves, emission can occur in the oxide as well as from the metal at the metal-oxide interface, yielding information about the oxide. This is the case for aluminum oxide on aluminum that had been ion bombarded with 2-kV Ar^+. For films that are emitting while the metal is not, information is gleaned about the film. This is the case for NiO/Ni in this study. Ellipsometry was used to relate photoemission to the thickness of the oxide film. Surface potential difference (SPD) measurements were also made for comparison with the photoemission measurements.

EXPERIMENTAL

A simple arrangement for measuring photoemission under ambient laboratory conditions is shown in Fig. 1(b). This technique was first reported by Hoenig[1] and Moore *et al.*[2] The grounded specimen is in series with a battery such that the Ohms guard on the back of the Keithly 600A electrometer is floating at 30 V positive with respect to ground. A reference electrode attached to the input of the electrometer is therefore at 30 V positive with respect to the sample emitter and acts as the electron collector. Our uv light source (Pen Ray) emits light primarily at 2500 Å. The input wire between the collector and the electrometer is shielded. The shield is connected to the electrometer ground connector but not to the collector.

The SPD is the difference between the work function of the sample ϕ and the work function of the reference electrode ϕ_{ref}, i.e.,

$$\mathrm{SPD} = \phi - \phi_{ref}. \tag{1a}$$

The SPD will be positive or negative depending on the work-function values. If the work function of the reference electrode remains constant, any change in SPD will be ascribed to changes in the sample work function, a positive change if ϕ increases and a negative change if ϕ decreases.

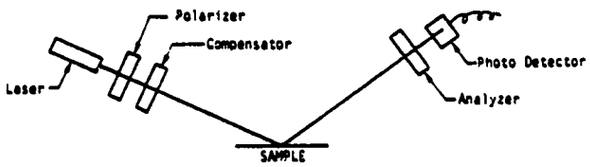

(a) ELLIPSOMETRY

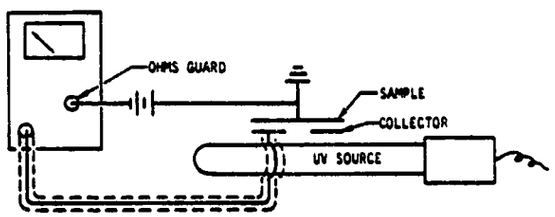

(b) PHOTO-EMISSION

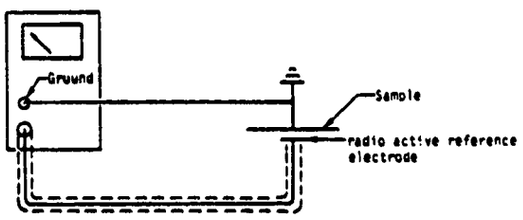

(c) SPD

FIG. 1. (a) Schematic diagram of the ellipsometer. (b) Schematic diagram of electrical circuit for measuring photoemission. (c) Schematic diagram of electrical circuit for measuring SPD.

TABLE I. Ellipsometric, SPD, and photoemission results for oxide films on Al.

Anodize (V)	Ellipsometric Δ	Ellipsometric ψ	Oxide thickness (Å)	κ	Photocurrent I_p (×10^{11} A)	I_p after ion bombardment (×10^{11} A)	SPD (V)	SPD after ion bombardment
				Anodized Al/Au/Cr/glass				
0	131.6	40.7	66	0.20	130.0		0.96	
3	123.6	40.9	115	0.13	20.5		1.46	
7	119.4	41.1	142	0.08	4.5		1.30	
14	107.7	41.4	230	0.05	0.3		1.46	
36	83.6	43.7	520	0.00	0.0		1.20	
							avg. 1.28 ± 0.16	
				Anodized 1100 Al plate				
0	133.6	41.2	55	0.13	3.5	11	0.81	0.22
7.1	113.6	41.5	185	0.05	0.9	9	1.30	1.1
35.7	83.0	43.8	510	0.0	0.0	4	0.90	0.6
35.7	82.9	43.8	501	0.0	0.0	6	1.40	0.6
35.7	82.5	44.0	547	0.0	0.0	5	0.90	0.7
71.4	−121.0	48.1	1078	0.0	0.0	5	1.05	1.05
71.4	−120.2	48.0	1080	0.0	0.0	5	1.40	1.2
							avg. 1.31 ± 0.25	
				Acid etch 1100 Al plate				
	110.6	32.5	190	0.3	1.2		0.63	
	107.3	33.8	210	0.3	0.8		0.78	
	103.7	34.4	240	0.3	1.0	13	0.81	0.07
	108.2	35.1	205	0.3	1.0	15	0.87	0.10
			avg. 211	0.3	1.0		0.77 ± 0.07	

The SPD between the sample and a reference electrode is measured as shown in Fig. 1(c). The current flowing through this circuit can be expressed as

$$i = \mathrm{SPD}/(R + r) = E/r, \qquad (1b)$$

where E is the electrometer reading, r is the internal resistance of the electrometer ($\sim 10^{14}\ \Omega$), and R is the air-gap resistance between the sample and the reference electrode. In order for SPD $\approx E$, R must be much smaller than r. This is accomplished by ionization of the air in the gap with α particles. A radioactive substance is sealed behind a thin foil of metal on the surface of the reference electrode to provide the α particles. To establish that $R \ll r$ and SPD $\approx E$, measurements are made as the reference electrode approaches the sample; when E becomes independent of distance between electrodes, $R \ll r$.

As an independent method of measuring film thickness, ellipsometry was used [Fig. 1(a)]. Details of the ellipsometric technique can be found in Ref. 3. The azimuth of the ellipsometer polarizer and analyzer yield the phase shift Δ and the amplitude ratio (tanψ) of the parallel and normal components of the reflected light. Our measurements were performed with a He-Ne laser ($\lambda = 6328$ Å) at an angle of incidence of 70°. Measurements were made in four zones and averaged. The complex refractive index can be expressed as $\hat{n} = n(1 - i\kappa)$, where n is the real part and κ the imaginary part (absorption index). Values for the substrates at $\lambda = 6328$ Å are $n_s \approx 1.43$ and $\kappa_s \approx 5.17$ for Al and $n_s \approx 1.82$ and $\kappa_s \approx 2.0$ for Ni.

To interpret the ellipsometric results, it is assumed that the oxide films have optical properties close to bulk-oxide properties. The index of refraction of bulk alumina and nickel oxide is $n_f \sim 1.7$ and 2.3, respectively. The absorption index κ_f of these materials is approximately zero (i.e., they are transparent to 6328-Å light). If solutions for film thickness cannot be found for $\kappa_f = 0$, we use the solution for which n_f is close to the bulk value and an effective value of κ_f. The effective value of κ_f is probably not a true absorption index but reflects the fact that surface roughness is playing a role and has not been taken into account.

Aluminum samples were prepared in three ways: (i) plates of commercial 1100 Al were electropolished and then anodized to varying oxide thickness, (ii) Al was vapor deposited onto glass plates prior to anodizing, and (iii) 1100 Al plates were acid etched in dichromate-sulfuric acid solutions. The electropolish solution was 200 ml of $HClO_4$ per liter of ethyl alcohol. Samples were electropolished for 2 min at 0.2 A/cm^2 at 20 V, 10 °C, and then thoroughly washed in MeOH. The anodize solution was 30 g of ammonium borate per liter of water with pH adjusted to 9 with ammonia.

The dichromate-sulfuric acid etch was performed by immersion in a dichromate-sulfuric acid solution for 13 min at 66 °C. The solution was 28.5 g of sodium dichromate and 285 g of sulfuric acid added to distilled water to make 1 liter. The solution had been reacted with Al metal to give a dark-brown color. The samples were spray rinsed with cold water, immersed in cold water and repeatedly spray rinsed, and then dried in an over at 40 °C for 15 min.

Al vapor was deposited to ~2000 Å thickness on glass slides after first depositing 200 Å of Cr and 1000 Å of Au in order to provide good adhesion of Al to the glass.

Nickel samples were prepared as ~0.050-in. sheet

TABLE II. Ellipsometry, SPD, and photoemission of NiO/Ni.

Side	Temperature (°C)	Time (h)	Δ	ψ	n	κ	Thickness (Å)	Photoemission ($\times 10^9$ A)	Photoemission ($\times 10^9$ A)	SPD (V)	SPD (V)
	Room		106.46	27.95	2.6	0.9	155	0.1	0.2	0.27	0.36
	200	3	113.04	30.8	2.6	1.0	71	0.5	0.7	−0.11	−0.06
X	200	3	113.30	28.7	2.6	1.3	71	0.45	0.8	0.08	−0.05
	500	1	108.4	26.1	2.6	1.3	150	2.1	2.2	−0.31	−0.30
X	500	1	68.8	29.9	2.6	0.25	250	2.7	3.2	−0.26	−0.26
						Polished slug of Ni					
	Room		118.3	33.2	2.6	0	~15	0.35		0.37	
	200	3	119.6	33.7	2.6	0	~15	0.35		0.17	
	300	1	112.9	33.8	2.6	0	40		1.4		0.13
	400	1	88.1	35.6	2.6	0	140		2.2		−0.21
	500	1	−81.0	41.7	2.6	0	590	2.7		−0.5	
	500	1	−134.4	21.1	2.6	0.08	870		2.5		−0.17
	500	4	111.6	21.5	2.6	0.8	1073		2.5		−0.20

and as thick polished slugs (~1 in. in diameter by ½ in. in depth). The oxide films were formed by heating in oxygen to various temperatures.

EXPERIMENTAL RESULTS

The Al_2O_3/Al system

Table I gives experimental results for ellipsometry, surface potential difference, and photoemission for Al_2O_3/Al.

Ellipsometry

For anodized oxide films on aluminum (vapor deposited or plate) the ellipsometric results yield $\kappa_f \sim 0$, $n_f \approx 1.7$, and a thickness ≈14 Å/V, if the oxide thickness is ≥ 500 Å. These results are in close agreement with the literature.[4] For thinner films, solutions for thickness ≈14 Å/V and $n_f \approx 1.7$ cannot be found unless the effective absorption index $\kappa_f > 0$. This effect is probably due to the increased effect surface roughness plays for very thin films, as indicated by the large value of κ_f for the very rough acid-etch plates.

Photoemission

The background photoemission current was 1.5×10^{-11} A; consequently, for films thicker than about 250 Å, where the current was near or less than this, meaningful measurements could not be made. Photocurrents reported in Table I are the measured values minus the background current. Therefore, the values of 0.0 reported in Table I refer to currents equal to or less than 1.5×10^{-11} A. Ion bombardment of the anodized 1100 Al plates and acid-etched plates caused a large increase in I_f that is approximately independent of film thickness above 500 Å. This result indicates that ion bombardment has reduced the threshold such that the oxide has become emitting. However, exposure of the bombarded oxide to the uv light caused the emission current to drift back toward the prebombardment value.

SPD

The surface potential difference is approximately independent of oxide film thickness for anodized Al (SPD ~1.3 V). Acid etching of Al decreases SPD to ~0.8 V. Ion bombardment also decreases SPD considerably with respect to the nonbombarded samples.

The NiO/Ni system

Table II gives the experimental results for ellipsometry, photoemission, and SPD for NiO/Ni.

Ellipsometry

Up to 580 Å the oxide on the polished Ni slug can be interpreted as transparent ($\kappa_f \sim 0$) to 6328-Å light if $n_f \approx 2.6$ (as compared to 2.3 for the bulk oxide). The values of Δ and ψ for the polished Ni slug, exposed to air at room temperature and 200 °C, are within one degree of the values for a clean Ni surface with optical constants $n_s \approx 1.82$ and $\kappa_s \approx 2.0$. The oxide film thickness is therefore extremely thin and is assumed to be about 15 Å as reported in the literature.[5] The cause of the larger value of κ_f for the thickest film (~1073 Å) on polished Ni is not known, unless longer oxidation times cause some roughening. The effective values of κ_f for sheet Ni are very large, probably reflecting the rough nature of the rolled sheet.

In Table II, for sheet Ni, side X refers to the side of the sheet adjacent to the ambient gas. The other side was adjacent to the support in the furnace. There was little difference in ellipsometric results between side X and the other side at 200 °C, but at 500 °C a large difference is noted. The thinner film on the under side is probably due to depletion of oxygen in that region. Comparison of the oxide thickness after exposure at the same temperature and time reveals that much thicker films are formed on the polished slug than the sheet. Note that heating the Ni sheet from room temperature to 200 °C decreases the film thickness. This is caused by the removal of a layer of organic contamination, as is evidenced by the photoemission and SPD results.

Photoemission

The two sets of data for photoemission and SPD, in Table II, were taken on two different days. The two sets of data show that the measurements were fairly reproducible and did not change with time. The photoemission results for NiO/Ni are completely different from those

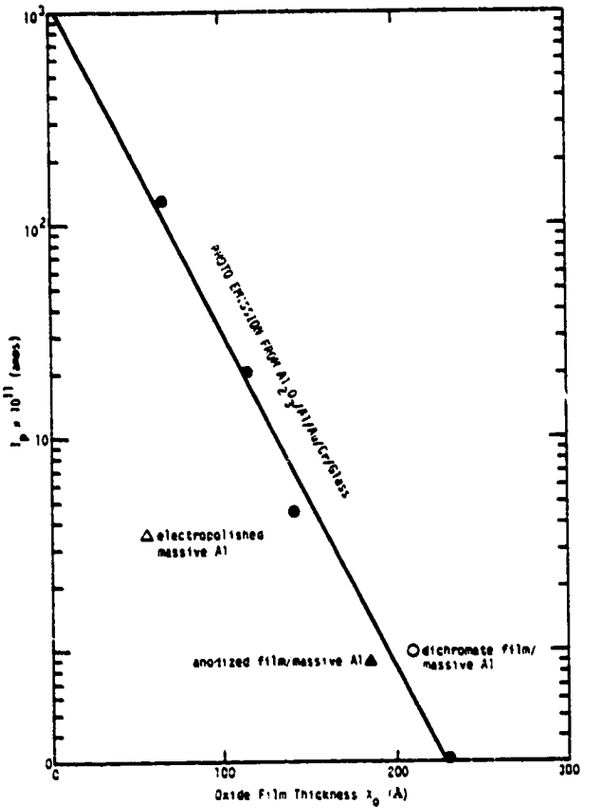

FIG. 2. Semilog plot of photoemission current I_p vs oxide film thickness Δx_0(Å). Solid points represent anodized vapor deposited Al, crosses represent the anodized Al 1100 plate, open circles represent the acid etched Al 1100 plate, and open triangles represent the electropolished Al 1100 plate.

for Al_2O_3/Al in that emission increases with oxide thickness. If the oxide was thicker at room temperature than at 200 °C, I_p at room temperature should be larger than at 200 °C. The fact that I_p is much smaller at room temperature indicates that either the emitting oxide is thinner or that a contamination layer is attenuating the emission. The latter explanation is consistent with the ellipsometric result of a net decrease in film thickness (but not oxide thickness) as the temperature was increased to 200 °C.

SPD

Contrary to the results for Al_2O_3/Al, the SPD for NiO/Ni changes with oxide thickness and changes from positive to negative with the removal of the contamination.

DISCUSSION AND CONCLUSIONS

Photoemission measurements are very simple to make under ordinary ambient conditions. By using the appropriate light wavelength, emission from the metal substrate can be separated from emission from the oxide layers. For interpretation of our results, let x be the distance in the oxide perpendicular to the plane of the substrate, $x=0$ at the gas-oxide interface and $x=x_0$ at the oxide-metal interface. It is assumed that attenuation of the light in the oxide as compared to total light flux is small for the oxide thicknesses under consideration. Let $P(x)$ be the escape probability of electrons from position x in the oxide, per unit length, averaged with respect to energy; N_p the number of incident photons per second; P_0 the probability of photon absorption at x in the oxide; P_m the probability of photon absorption in the metal; Y_0 the number of emitted electrons per absorbed photon in the oxide; Y_m the number of emitted electrons per absorbed photon in the metal; and G the fraction of emitted electrons that are collected (includes geometric and field effects due to imposed potential between sample and collector). The probability that an electron will escape from position x in the oxide can be expressed in exponential form[6] as

$$P(x)=C_0\exp(-\bar{x}'/L). \tag{2}$$

where C_0 is a factor that depends on the work function of the oxide and L is the attenuation length, characteristic of the average energy of the exited electrons. x' is the distance along the direction θ with respect to the surface normal (i.e., $x'=x/\cos\theta$). The average distance $\bar{x}'$ is

$$\bar{x}'=\left[\int_{-\theta_0}^{\theta_0}(x/\cos\theta)\,d\theta\right]/2\theta_0, \tag{3}$$

where electrons are collected within solid angle Ω about θ_0. Equation (2) becomes

$$P(x)=C_0\exp(-x/L), \tag{4}$$

where

$$L'=L\ln\frac{\tan(\frac{1}{4}\pi+\frac{1}{2}\theta_0)}{\tan(\frac{1}{4}\pi-\frac{1}{2}\theta_0)}\,. \tag{5}$$

The photocurrent I_p can be expressed as

$$I_p=\left[\int_0^{x_0/L'}GN_pP_0Y_0P(x)\,d(x/L')\right]+GN_pP_mY_mP(x_0), \tag{6}$$

where the first term on the right-hand side of Eq. (6) is for electron emission from the oxide and the second term is for emission from the metal. Integration of Eq. (6) after substituting for $P(x)$ from Eq. (4) yields

$$I_p=GN_pC_0P_0Y_0[1-\exp(-x_0/L')]+P_mY_m\exp(-x_0/L'). \tag{7}$$

Collecting constants, Eq. (7) becomes

$$I_p=I_{p0}^0[1-\exp(-x_0/L')]+I_{pm}^0\exp(-x_0/L'), \tag{8}$$

where

$$I_{p0}^0=GN_pC_0P_0Y_0 \tag{9}$$

$$I_{pm}^0=GN_pC_0P_mY_m. \tag{10}$$

At $x_0\ll L'$, $I_p=I_{pm}^0$, and at $x_0\gg L'$, $I_p=I_{p0}^0$.

The relationship between C_0 and the oxide work function is found in the Fowler equation[7] for saturated emission, i.e.,

$$C_0\propto T^2f(\Delta)(w_a-h\nu)^{-1/2}, \tag{11}$$

where T is the absolute temperature and w_a is the energy to remove electrons if they are at rest. For $\Delta\leq 0$,

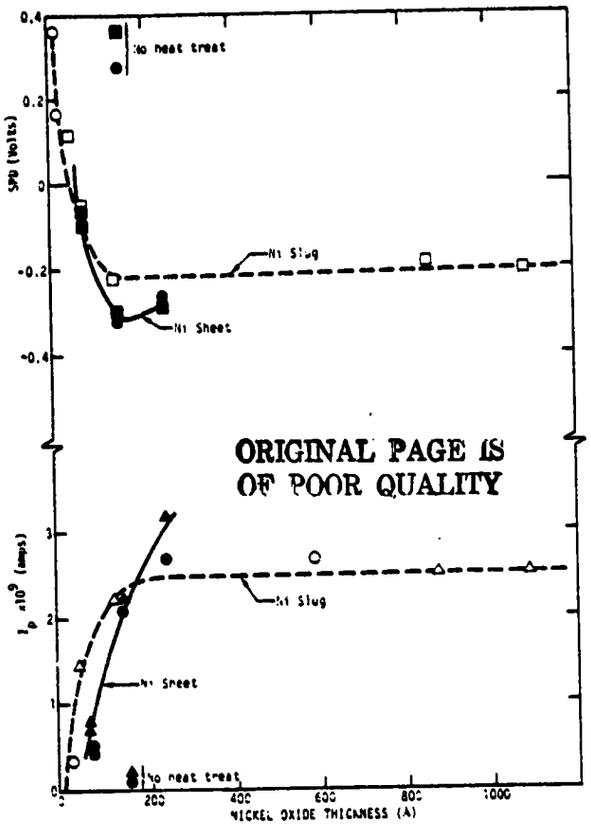

FIG. 3. Plot of I_p and SPD for NiO/Ni vs thermal oxide thickness. The open circles and open triangles represent the polished Ni slugs measured on different days. The solid points and squares represent the Ni sheet.

$$f(\Delta)=e^{\Delta}-\frac{e^{2\Delta}}{2^2}+\frac{e^{3\Delta}}{e^3}-\cdots\cdots, \tag{12}$$

and for $\Delta \geq 0$,

$$f(\Delta)=\left[\frac{\pi^2}{6}+\frac{\Delta^2}{2}-\left(e^{-\Delta}-\frac{e^{-2\Delta}}{2^2}+\frac{e^{-3\Delta}}{3^3}-\cdots\right)\right] \tag{13}$$

$$\Delta=(h\nu-e\phi)/kT, \tag{14}$$

where k is the Boltzman constant and ϕ is the work function. For the electrical circuit of Fig. 1(b), the work function is related to the surface potential difference by

$$\mathrm{SPD}=\phi-\phi_{\mathrm{ref}}, \tag{15}$$

where ϕ_{ref} is the work function of the reference electrode. The reference electrode was a Ni foil (with thin natural oxide layer).

The Al_2O_3/Al system

For Al_2O_3 Al, emission occurs from the metal because the photoelectric threshold is 4.2 eV and the light we used was about 5 eV. Photoemission does not occur from the oxide because the photoelectric threshold (the work function) is about[8] 8 eV. Therefore, for Al_2O_3/Al, $P_0 \approx 0$ and Eq. (7) reduces to

$$I_p \approx I_{pm}^0 \exp(-x/L'). \tag{16}$$

The data from Table I are plotted in Fig. 2 on semilog paper according to Eq. (16). The solid circles in Fig. 2 represent the anodized Al that had been vapor deposited on glass, the solid triangle represents the anodized Al (1100) plate, the open circle represents the acid-etched Al (1100) plate, and the open triangle represents the electropolished Al (1100) plate. All of the data in Fig. 2 fall close to the straight line drawn through the data points except for the electropolished sample. This indicates that either the values of I_{pm}^0 or L' are different for the electropolished film than for the others and is probably due to structural differences in this film. From Fig. 2, except for the electropolish film, $I_{pm}^0 \approx 1.1\times10^{-8}$ A and $L' \approx 28$ Å. The fact that I_{pm}^0 is a constant indicates from Eqs. (10) to (15) that the SPD is constant. Values of SPD for anodized Al are approximately constant, independent of thickness (see Table I).

The average electron energy associated with L' is not known; however, for a given photon energy the maximum initial energy E_m would be[6] $h\nu-(\phi_b+E_c)$, where E_0 is the electron affinity of the oxide and ϕ_b is the energy barrier at the Al-Al_2O_3 interface. Pong[6] estimates $\phi_b \approx 1.4\pm0.7$ eV and $E_0 \approx 1$ eV. Therefore, for $h\nu \approx 5$ eV ($\lambda = 2500$ Å), the maximum initial energy of electrons emitted into the oxide would be $E_m \approx 2.6$ eV. Kanter and Feibelman[9] measured L' at approximately the same initial energy ($E_m \approx 3$ eV). Our value for L' of 28 Å is in close agreement with their value of 25 Å. For much larger initial energy ($E_m \approx 7.8$ eV) Pong[6] obtained a value of $L' \approx 130\pm30$ Å.

The positive value of SPD, 1.3 V, for anodized Al plates or vapor deposited Al is approximately independent of oxide thickness and indicates that $\phi(Al_2O_3/Al) - \phi(\text{Ni foil}) \approx 1.3$ eV. Since the work function of the reference is stable, the decrease of ~(0.2–0.3) V in SPD after ion bombardment is attributed to a decrease in $\phi(Al_2O_3/Al)$. A corresponding increase in I_0 is attributed to electron emission from the oxide after bombardment. The approximately constant value of $I_p \approx 5\times10^{-11}$ A after ion bombardment of anodized Al 1100 plate, independent of oxide thickness, indicates that ion damage is restricted to a thin outer layer. The large decrease of $\phi(Al_2O_3/Al)$ (~0.8 eV) due to ion bombardment for the electro-polished and acid-etched samples (large κ_f) causes a large increase in I_p.

The NiO/Ni system

For NiO/Ni, emission from the metal is very small because the photoelectric threshold is close to the energy of the light used (~5 eV). The data in Table II are plotted in Fig. 3. The value of $I_p \approx 0$ at $x_0 \approx 0$, but increases with increasing film thickness. This shows that photoemission is from the oxide in spite of the fact that the photoelectric threshold is about[8] 5.3 eV. Since photoemission does occur from NiO, the oxide film on Ni must have a threshold lower than reported[8] for bulk oxide.

For NiO/Ni, $P_m Y_m$ is small and Eq. (8) reduces to

$$I_p \approx I_{p0}^0[1-\exp(-x_0/L')]. \tag{17}$$

From Fig. 3 for the polished Ni slug,

$I_{p0}^{0} \approx 2.5 \times 10^{-9}$

$L' \approx 71$ Å.

As mentioned before, the curve of I_p vs oxide thickness for Ni sheet is probably shifted to the right, in Fig. 3, due to nonemitting contamination. However, it is apparent that for Ni sheet, $I_{p0}^{0} \sim 3 \times 10^{-9}$ A. The value for SPD for NiO/Ni should be small, as observed in Table II, because the reference electrode is also NiO/Ni. The work function of the NiO/Ni decreases as the film thickness increases, dropping below that of the reference electrode at about 50 Å. There is a correlation between SPD and I_p for NiO/Ni; as the work function of the oxide decreases the photo current increases. However, this correlation may or may not be direct. It has been assumed in deriving I_{p0}^{0} and L' for NiO/Ni that I_{p0}^{0} is constant. The validity of this assumption depends on the value of Δ of Eq. (14) (therefore, ϕ). According to Eqs. (12) and (13), if $e\phi \approx h\nu$, $f(\Delta) \approx$ constant, in which case I_{p0}^{0} is constant. If $e\phi$ is not $\approx h\nu$, then I_{p0}^{0} is not a constant and the value of L' will be modified.

It is concluded that the measurement of photoemitted electrons from a metal-film system are simple to perform under ordinary laboratory conditions and that these measurements can be useful for estimating the thickness of very thin oxide films (0—200 Å) if calibration curves such as Figs. 2 and 3 have been made.

ACKNOWLEDGMENT

The NiO/Ni samples were provided by W.M. Robertson and the Al was anodized by R.S. Spurling.

[1] S.A. Hoenig, Air Force Materials Laboratory Report No. AFML-TR-71-140, Part 1, 1971 (unpublished).
[2] J.F. Moore, S. Tsang, and G. Martin, Air Force Materials Laboratory Report No. AFML-TR-71-185, 1971 (unpublished).
[3] F.L. McCrackin, E. Passaglia, R. Stromberg, and H.L. Steinberg, J. Res. Natl. Bur. Stand. (U.S.) A 67, 363 (1963).
[4] S. Tajima, *Advances in Corrosion Science and Technology*, edited by M.G. Fontana and R.W. Staehle (Plenum Press, New York, 1970), Vol. 1, p. 234.
[5] O. Kubaschewski and B.E. Hopkins, *Oxidation of Metals and Alloys* (Butterworths, London, 1962).
[6] W. Pong, J. Appl. Phys. 40, 1733 (1969).
[7] L.B. Loeb, *Basic Processes of Gaseous Electronics* (University of California Press, 1961), p. 666.
[8] R.J. Powell, U.S. Army Research Office, Durham, N.C., Technical Report No. 5220-1 (SU-SEL-67-032), Contract No. DA31 124ARO(d)430, 1967 (unpublished).
[9] H. Kanter and W.A. Feibelman, J. Appl. Phys. 33, 3550 (1962).